Published in Applied Physics Letters 112, issue 11, 113502-1/5, 2018
which should be used for any reference to this work

Study of additive manufactured microwave cavities for pulsed optically pumped atomic clock applications

C. Affolderbach,[1,a),b)] W. Moreno,[1,b)] A. E. Ivanov,[2] T. Debogovic,[3] M. Pellaton,[1] A. K. Skrivervik,[2] E. de Rijk,[3] and G. Mileti[1,a)]
[1]*Laboratoire Temps-Fréquence (LTF), Institut de Physique, University of Neuchâtel, Avenue de Bellevaux 51, 2000 Neuchâtel, Switzerland*
[2]*Microwave and Antenna Group (MAG), École Polytechnique Fédérale de Lausanne, 1015 Lausanne, Switzerland*
[3]*SWISSto12 SA, EPFL Innovation Park Building L, Chemin de la Dent d'Oche 1B, 1024 Ecublens, Switzerland*

Additive manufacturing (AM) of passive microwave components is of high interest for the cost-effective and rapid prototyping or manufacture of devices with complex geometries. Here, we present an experimental study on the properties of recently demonstrated microwave resonator cavities manufactured by AM, in view of their applications to high-performance compact atomic clocks. The microwave cavities employ a loop-gap geometry using six electrodes. The critical electrode structures were manufactured monolithically using two different approaches: Stereolithography (SLA) of a polymer followed by metal coating and Selective Laser Melting (SLM) of aluminum. The tested microwave cavities show the desired TE_{011}-like resonant mode at the Rb clock frequency of ≈6.835 GHz, with a microwave magnetic field highly parallel to the quantization axis across the vapor cell. When operated in an atomic clock setup, the measured atomic Rabi oscillations are comparable to those observed for conventionally manufactured cavities and indicate a good uniformity of the field amplitude across the vapor cell. Employing a time-domain Ramsey scheme on one of the SLA cavities, high-contrast (34%) Ramsey fringes are observed for the Rb clock transition, along with a narrow (166 Hz linewidth) central fringe. The measured clock stability of 2.2×10^{-13} $\tau^{-1/2}$ up to the integration time of 30 s is comparable to the current state-of-the-art stabilities of compact vapor-cell clocks based on conventional microwave cavities and thus demonstrates the feasibil-ity of the approach.

Compact microwave atomic clocks[1] based on alkali vapor cells[2,3] are widely employed as stable frequency references in numerous applications, ranging from telecommunication networks[4] to onboard clocks in satellite navigation systems.[5,6] In such atomic clocks, the frequency of a quartz local oscillator is stabilized to an inherently stable microwave transition in an alkali atom vapor held in a vapor cell. This greatly suppresses the quartz's fractional frequency instabilities to the 10^{-12} to $<10^{-14}$ range (timing accuracies of 0.1 μs to <1 ns, respectively) over timescales up to one day. During the last decade, thanks to the employment of laser optical pumping, important advances were made in vapor-cell Rb atomic clocks based on the double-resonance (DR) scheme, using both the continuous-wave (CW)[7] and the pulsed optical pumping (POP) interrogation (Ramsey scheme),[8,9] where the pulsed Ramsey scheme is of particular interest for highly compact and high-performance Rb cell clocks. In all types of DR atomic clocks, the microwave resonator cavity is a critical component for applying the microwave field to the atoms in a well-controlled geometry. In view of practical applications, this microwave cavity should be small and light-weight and feature simple and fast assembly. In DR atomic clocks, such cavities are generally manufactured by conventional subtractive precision machining of metals, often followed by time-consuming assembly steps requiring precise positioning or alignment of the cavity components.

During the past few years, tremendous progress has been made in the field of additive manufacturing (AM), with several AM techniques nowadays available for manufacturing of microwave components.[10] Two AM techniques are especially suitable for the fabrication of microwave cavities: Stereolithography (SLA) and Selective Laser Melting (SLM). Recently, complex waveguide-based microwave components made by SLA of polymers followed by metal coating were reported,[11] and first simple microwave resonator structures made by SLM of aluminum were demonstrated.[12] It is of interest to exploit AM of microwave cavities for atomic clocks that exhibit more complex geometries,[13] to simplify manufacture and assembly, and—in the case of SLA of polymers—reduce the cavity mass. Recently, we reported on the proof-of-principle realization of a compact microwave cavity for CW-DR atomic clocks using SLA of a polymer.[14] Here, we report on the detailed characterization of such AM cavities, manufactured by either SLA of a polymer or SLM of aluminum, and their implementation to high-performance Rb atomic clocks in the Ramsey scheme.[8]

In a Rb vapor-cell atomic clock,[2,3] the reference "clock" transition is given by the $5S_{1/2}$ $|F = 1, m_F = 0\rangle \leftrightarrow |F = 2, m_F = 0\rangle$ magnetic dipole transition at ≈6.835 GHz. Shifting

a)Authors to whom correspondence should be addressed: christoph.affolderbach@unine.ch and gaetano.mileti@unine.ch.
b)C. Affolderbach and W. Moreno contributed equally to this work.

only in second order with an external static magnetic field, the clock transition is conveniently isolated from the other m_F Zeeman transitions by applying such a field (field vector $\boldsymbol{B}_{\mathrm{dc}}$) that defines the quantization axis. Driving the clock transition requires the microwave magnetic field vector $\boldsymbol{H}$ to be parallel to the quantization axis, which in Rb atomic clocks generally is collinear with the laser propagation vector $\boldsymbol{k}$ (see Fig. 1). In practical realizations, the vapor cell and microwave cavity often have cylindrical geometry.[13,15] Two main requirements apply to the cavity field mode: first, in order to obtain a strong clock transition signal, $\boldsymbol{H}$ should be perfectly parallel to the quantization axis ($\boldsymbol{B}_{\mathrm{dc}}$) throughout the vapor cell; second, in particular for the POP clock mode,[8,9] the microwave field amplitude should be as homogeneous as possible throughout the cell such that for a given microwave pulse duration, as many atoms as possible undergo an ideal $\pi/2$-pulse on the clock transition.

Our cavity is based on the so-called loop-gap structure[13,16] which, for the used TE_{011}-like mode, has a magnetic field distribution favorable for clock operation [Fig. 1(a)]. In a simplified way, it can be modelled via its equivalent lumped elements where the equivalent capacitance (reactance) can be considered as mainly dependent on the gap geometry, such as the gap width and thickness, as well as electrode height [Fig. 1(b)], while the equivalent inductance is mainly attributed to the cavity radius [see Eq. (1) in Ref. 13] The two parameters being geometrically decoupled allows us to significantly reduce the cavity radius, for a given frequency, by compensating the change in the reactance with the gap size. The result is a compact device with approximately three times lower volume compared to a simple cylindrical geometry.[15] The field homogeneity of such cavities was previously studied experimentally[17] and theoretically,[18] where the loop-gap approach was found to perform on a par with the standard cylindrical geometry. The quality of field orientation can be evaluated by the Field Orientation Factor (FOF),[13] obtained by numerical simulations as $\mathrm{FOF} \approx 0.9$, over the whole cell volume. Obviously, a high FOF can be achieved if the regions where the field lines turn

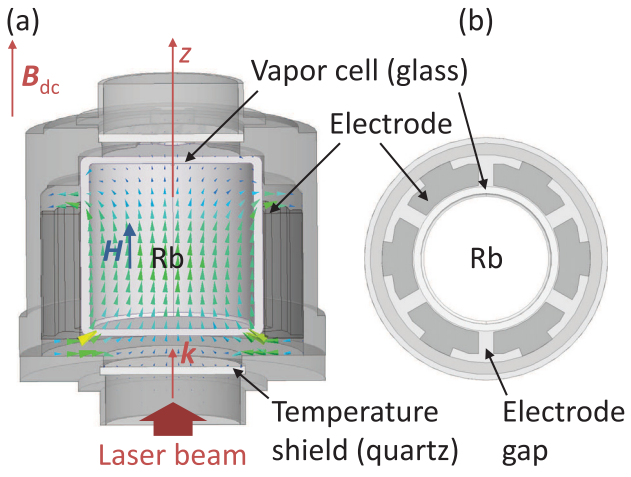

FIG. 1. (a) Cavity design view shown with the numerically simulated magnetic field distribution (colored arrows) and the field geometry required for clock interrogation. (b) Electrode configuration: cut view perpendicular to the z axis.

are located outside the active volume of the Rb cell [see Fig. 1(a)]. Simulated Q-factors for the cavity are typically $\mathrm{Q} \approx 150$, dominated by losses in the dielectric cell walls.

Manufactured AM cavity cylinders are shown in Fig. 2. Both prototype cylinders are monolithic, combining the cylindrical shield and the electrode structure, thereby eliminating the need for time-consuming assembly and adjustments. Both cavity realizations are compatible with the same Rb cell and cavity endcaps equipped with the excitation loop. The aluminum cylinder (AlSi10Mg alloy, left-hand side of Fig. 2) is made using SLM and passivated with Alodine 1200s. No actions were taken to reduce the surface roughness of the cylinder (≈4–5 times larger for SLM compared to SLA) because RF losses are dominated by the dielectric cell walls and not by the roughness or bulk conductivity of the material. The polymer cylinder[14] (right-hand side of Fig. 2) is made using SLA. In order to become RF-functional, the cylinder body was metal-coated with copper using a proprietary electroless plating process of SWISSto12. This copper layer is homogeneous and sufficiently thick (>7 skin-depths) on all surfaces of the polymer body. A thin silver layer added on top of the copper layer ensures passivation. The masses of the aluminum and polymer cylinders are 86 g and 60 g, respectively. The polymer cylinder also benefits from a slightly better manufacturing precision of SLA (≈40 μm). One possible drawback of the SLA cylinder could be its lower thermal conductivity, with impact on cell temperature control. Inserts (SLA) and threads (SLM) serve for attaching the cavity bottom and could become obsolete in a future fully monolithic AM cavity.

The S_{11} parameter (return loss) was measured using a Vector Network Analyzer for the fully assembled SLA and SLM prototypes, see Fig. 3. The measured S_{11} parameters show that both realizations meet the required 6.835 GHz frequency, confirming well the simulations. Potential small frequency shifts, due to fabrication tolerances in the AM process or of the vapor cell, can be compensated by frequency tuning, mainly achieved using a set of prototypes with gap sizes varied in 50 μm steps. The use of this main design parameter is limited, however, by the presence of a nearby unwanted mode which can couple closer to the TE_{011}-like mode. Fine tuning of each cavity's resonance frequency is achieved by varying the dielectric loading of the cavity via adjusting the cell

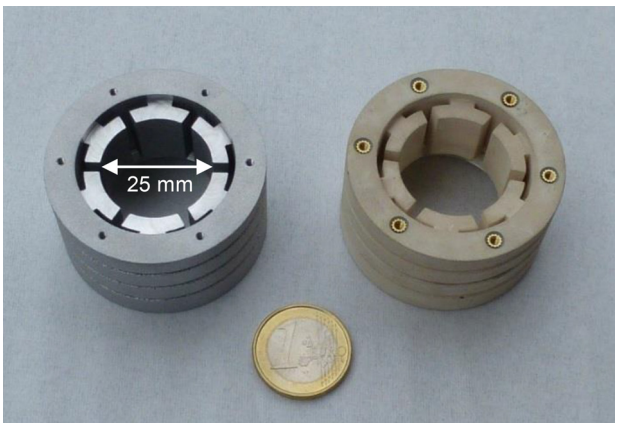

FIG. 2. Photograph of microwave cavity cylinders manufactured using SLM (aluminum, left) and using SLA (metal-coated polymer, right), next to a one-Euro coin.

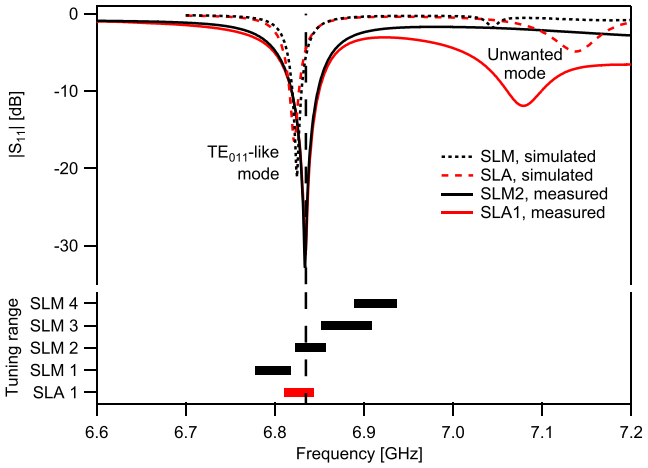

FIG. 3. Top: Measured (solid lines) and simulated (dashed lines) S_{11} curves for the SLM (black) and SLA (red) cavities. Due to calibration differences in the AM processes, the nominal gap sizes of prototypes SLA1 and SLM2 differ by 50 μm. Bottom: Measured frequency tuning ranges. Frequency tuning between the four SLM cavities (black bars) is achieved by gap sizes differing by 50 μm each. Frequency fine tuning of each single cavity, over the frequency range indicated by the widths of the horizontal bars, is achieved by varying the dielectric loading of the cavity via adjusting the cell position.

position. A sufficiently large tuning range is found, allowing us to meet the resonance condition for both cavity types (see Fig. 3). The measured Q-factors are ≈70 for the SLM and ≈60 for the SLA cavity, which are sufficient for our application. The difference to the simulated Q ≈ 150 is mainly attributed to manufacturing tolerances of the vapor cell (causing higher losses) as well as production uncertainties on the feeding loop, which can lead to increased coupling of the unwanted mode. The temperature-dependent shift of the cavity resonance frequency is measured as ≈−250 kHz/K, reasonably small for limiting clock instability contributions arising from cavity temperature fluctuations via cavity pulling.[1]

For testing in an experimental Rb clock,[9] the SLA cavity is heated to ≈57 °C and a dc coil placed around the cavity generates a field $\boldsymbol{B}_{\mathrm{dc}}$ collinear with the symmetry axis of the cavity (z in Fig. 1). The openings at both ends of the cavity allow the laser light, provided by a compact laser head emitting at 780 nm (Rb D2 line),[19] to travel through the cell, with $\boldsymbol{k}$ also parallel to the symmetry axis z. For all measurements presented here, the laser frequency was stabilized to the $F_g = 2 \leftrightarrow F_e = 3$ Doppler-free resonance obtained from an auxiliary evacuated Rb vapor cell integrated in the laser head. The whole cavity assembly is placed inside a mu-metal enclosure. The quality of the microwave magnetic field orientation ($\boldsymbol{H}$ parallel to $\boldsymbol{B}_{\mathrm{dc}}$) is evaluated in terms of the FOF (see Refs. 13 and 20 for the definition). Figure 4 shows a measurement of all seven Zeeman transitions in the ground state. The barely distinguishable sigma transitions induced by components of $\boldsymbol{H}$ perpendicular to $\boldsymbol{B}_{\mathrm{dc}}$[21] testify a highly uniform magnetic field, with an experimentally measured FOF = 0.98. The nearby presence of the unwanted mode (Fig. 3) thus does not degrade the field uniformity. The homogeneity of the longitudinal component H_z of $\boldsymbol{H}$ throughout the cell can be experimentally assessed via the damping of the atomic population's Rabi oscillations.[9] Figure 5 shows a comparison of Rabi oscillations measured for the SLA cavity and for a classically machined aluminum

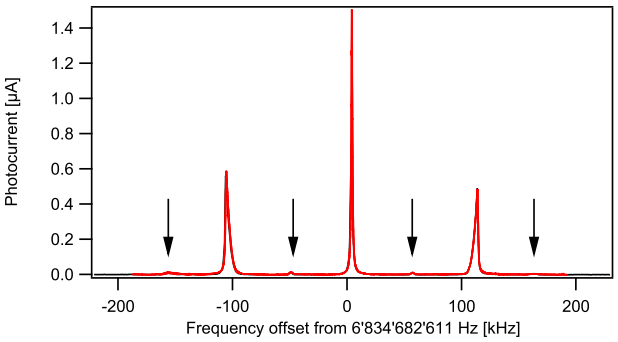

FIG. 4. DR spectrum of all possible Zeeman transitions, measured for the SLA cavity. The low-amplitude sigma-transitions are marked by arrows.

cavity, in terms of the normalized change in absorption R.[9] The slower damping observed for the SLA cavity demonstrates a better microwave field homogeneity across the cell. In both cases, data were taken using a Ramsey-type pulse sequence with a Ramsey time of $T_R = 3.0$ ms, and the microwave pulse area indicated refers to the total pulse area of the two nominal $\pi/2$ microwave pulses together.

For further evaluation, we operate the Rb atomic clock prototype in the POP scheme.[8,9] The duration of each pulse is set as follows: both optical pumping time and microwave pulse time: 0.4 ms, Ramsey time: 3 ms, and optical detection time: 0.9 ms. The total cycle period is 5.22 ms (including dead times). The quartz oscillator is frequency stabilized to the central fringe of the detected high-contrast Ramsey pattern shown in Fig. 6.

From the measured detection noise during the detection phase (see the inset in Fig. 7), we estimate a signal-to-noise limit for the clock stability of $1.1 \times 10^{-13}\ \tau^{-1/2}$.[22] The shot-noise instability limit is estimated to be $2.7 \times 10^{-14}\ \tau^{-1/2}$. An additional instability contribution of $7 \times 10^{-14}\ \tau^{-1/2}$ (Ref. 8) arises from the microwave synthesizer used[7] due to the Dick effect[23] for our modulation frequency of ≈200 Hz. Taking into account both the signal-to-noise limit and the Dick effect, an overall clock stability of $1.3 \times 10^{-13}\ \tau^{-1/2}$ is expected. The measured clock frequency stability is $2.2 \times 10^{-13}\ \tau^{-1/2}$ up to an integration time of 30 s, in good agreement with the expected stability (Fig. 7). This result is

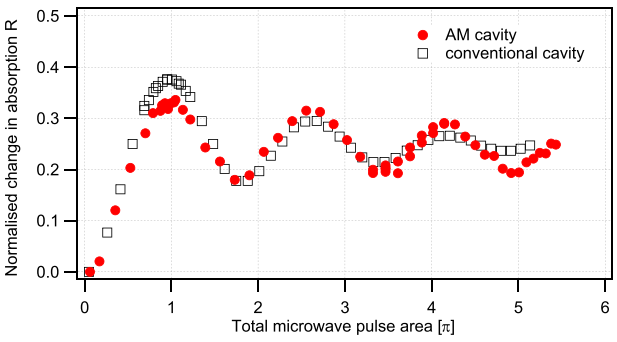

FIG. 5. Rabi oscillations observed with the SLA cavity (red filled circles), compared to the same data obtained with a cavity manufactured by classical techniques (black open squares).[9,13] The total microwave pulse area refers to the combined area of the two nominal $\pi/2$ microwave pulses in the Ramsey scheme employed here and is measured by the product of the total microwave pulse duration and the square root of microwave power. The pulse area is normalized such that the first maximum of the oscillation occurs at π.

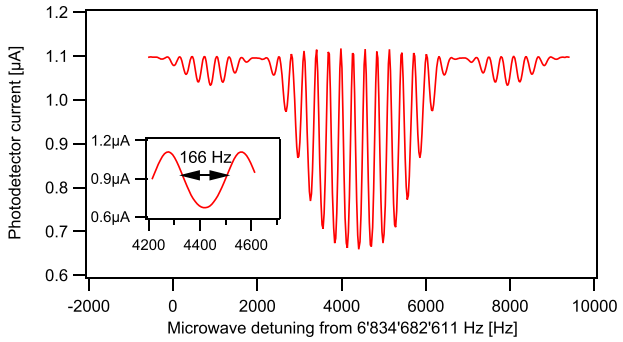

FIG. 6. Ramsey pattern measured with the SLA cavity. The central fringe linewidth is 166 Hz, corresponding to the 3.0 ms Ramsey time, and its contrast is 34%.

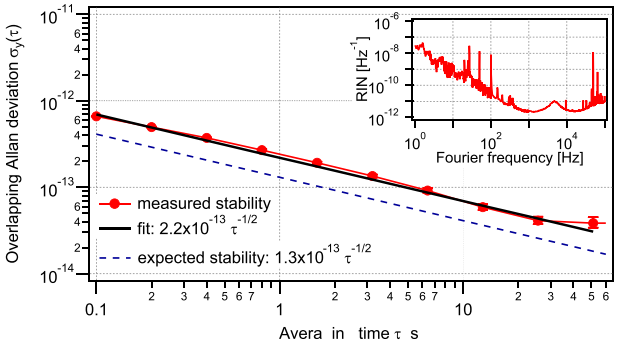

FIG. 7. Measured clock stability in the Ramsey mode. Inset: signal noise for the detection phase.

more than four times better than the one previously demonstrated using continuous-wave interrogation[14] and is comparable to the state-of-the-art clock stabilities reported for Rb DR atomic clocks operating in the pulsed[8] or CW[9] scheme.

In conclusion, we presented a detailed study of a compact loop-gap microwave resonator cavity realized by AM techniques, in view of its applications to high-performance vapor-cell atomic clocks. In spite of the somewhat limited spatial resolution of the AM processes, a good reproducibility of the critical cavity structures is obtained. The high FOF and clear Rabi oscillations measured demonstrate the good performances of the AM cavity in view of both the desired high degrees of uniformity and the homogeneity of the microwave magnetic field. The clock stability of 2.2×10^{-13} $\tau^{-1/2}$ measured in the pulsed Ramsey mode shows that AM microwave cavities can fulfill the stringent requirements for high-performance Rb vapor-cell clocks based on Ramsey operation, including for space applications.

This work was supported by Space Positioning Measures of the Swiss Space Office of the State Secretariat for Education, Research and Innovation of the Swiss Confederation (SERI/SSO), call 2016. The authors also acknowledge support of the Swiss National Science Foundation, Grant Nos. 156621 and 162346, as well as previous support of the European Space Agency (ESA) and the European Metrology Research Programme (EMRP Project IND55-Mclocks). The EMRP is jointly funded by the EMRP participating countries within EURAMET and the European Union. C.A., W.M., M.P., and G.M. thank C. E. Calosso (INRIM, Italy) for providing and support on the microwave local oscillator and F. Gruet and P. Scherler (both LTF, University of Neuchâtel, Switzerland) for support on the laser source and clock physics package.

[1]J. Vanier and C. Audoin, *The Quantum Physics of Atomic Frequency Standards* (A. Hilger, Philadelphia, USA, 1989).
[2]J. Camparo, "The Rb atomic clock and basic research," Phys. Today **60**(11), 33 (2007).
[3]J. Vanier and C. Mandache, "The passive optically pumped Rb frequency standard: The laser approach," Appl. Phys. B **87**, 565 (2007).
[4]J. A. Kusters and C. A. Adams, "Performance requirements of communication base station time standards," RF Des. **22**, 28–38 (1999).
[5]T. Dass, G. Freed, J. Petzinger, J. Rajan, T. J. Lynch, and J. Vaccaro, "GPS clocks in space: Current performance and plans for the future," in *Proceedings of 34th Annual Precise Time and Time Interval (PTTI) Meeting*, Reston, Virginia, 03–05 December (2002), pp. 175–192.
[6]P. Waller, F. Gonzalez, J. Hahn, S. Binda, R. Piriz, I. Hidalgo, G. Tobias, I. Sesia, P. Tavella, and G. Cerretto, "In-orbit performance assessment of GIOVE clocks," in *Proceedings of 40th Annual Precise Time and Time Interval (PTTI) Meeting*, Reston, Virginia, 1–4 December (2008), pp. 69–82.
[7]T. Bandi, C. Affolderbach, C. Stefanucci, F. Merli, A. K. Skrivervik, and G. Mileti, "Compact high-performance continuous-wave double-resonance rubidium standard with 1.4×10^{-13} $\tau^{-1/2}$ stability," IEEE Trans. Ultrason. Ferroelectr. Freq. Control **61**, 1769–1778 (2014).
[8]S. Micalizio, C. E. Calosso, A. Godone, and F. Levi, "Metrological characterization of the pulsed Rb clock with optical detection," Metrologia **49**, 425–436 (2012).
[9]S. Kang, M. Gharavipour, C. Affolderbach, F. Gruet, and G. Mileti, "Demonstration of a high-performance pulsed optically pumped Rb clock based on a compact magnetron-type microwave cavity," J. Appl. Phys. **117**, 104510 (2015).
[10]F. Calignano, D. Manfredi, E. P. Ambrosio, S. Biamino, M. Lombardi, E. Atzeni, A. Salmi, P. Minetola, L. Iuliano, and P. Fino, "Overview on additive manufacturing technologies," in Proc. IEEE **105**(4), 593–612 (2017).
[11]A. I. Dimitriadis, T. Debogovic, M. Favre, M. Billod, L. Barloggio, J. P. Ansermet, and E. de Rijk, "Polymer-based additive manufacturing of high performance waveguide and antenna components," Proc. IEEE **105**(4), 668–676 (2017).
[12]D. L. Creedon, M. Goryachev, N. Kostylev, T. B. Sercombe, and M. E. Tobar, "A 3D printed superconducting aluminium microwave cavity," Appl. Phys. Lett. **109**, 032601 (2016).
[13]C. Stefanucci, T. Bandi, F. Merli, M. Pellaton, C. Affolderbach, G. Mileti, and A. K. Skrivervik, "Compact microwave cavity for high performance rubidium frequency standards," Rev. Sci. Instrum. **83**, 104706 (2012).
[14]M. Pellaton, C. Affolderbach, A. K. Skrivervik, A. E. Ivanov, T. Debogovic, E. de Rijk, and G. Mileti, "3D printed microwave cavity for atomic clock applications: Proof of concept," Electron. Lett. (submitted).
[15]A. Godone, S. Micalizio, F. Levi, and C. Calosso, "Microwave cavities for vapor cell frequency standards," Rev. Sci. Instrum. **82**, 074703 (2011).
[16]W. Froncisz and J. S. Hyde, "The loop-gap resonator: A new microwave lumped circuit ESR sample structure," J. Magn. Reson. **47**, 515–521 (1982).
[17]C. Affolderbach, G.-X. Du, T. Bandi, A. Horsley, P. Treutlein, and G. Mileti, "Imaging microwave and DC magnetic fields in a vapor-cell Rb atomic clock," IEEE Trans. Instrum. Meas. **64**(12), 3629–3637 (2015).
[18]A. E. Ivanov, C. Affolderbach, G. Mileti, and A. K. Skrivervik, "Design of atomic clock cavity based on a loop-gap geometry and modified boundary conditions," Int. J. Microwave Wireless Technol. **9**, 1373–1386 (2017).
[19]S. Kang, M. Gharavipour, F. Gruet, C. Affolderbach, and G. Mileti, "Compact and high-performance Rb clock based on pulsed optical pumping for industrial applications," in *Proceedings of the 2015 Joint Conference of the IEEE International Frequency Control Symposium and the European Frequency and Time Forum*, Denver, USA, 12–16 April 2015 (IEEE, New York, 2015), pp. 800–803.
[20]M. Violetti, M. Pellaton, C. Affolderbach, F. Merli, J.-F. Zürcher, G. Mileti, and A. K. Skrivervik, "The microloop-gap resonator: A novel miniaturized microwave cavity for double-resonance rubidium atomic clocks," IEEE Sens. J. **14**(9), 3193–3200 (2014).
[21]M. Pellaton, Ph.D. thesis, Université de Neuchâtel, Neuchâtel, Switzerland, 2014.

[22]S. Kang, M. Gharavipour, C. Affolderbach, and G. Mileti, "Stability limitations from optical detection in Ramsey-type vapour-cell atomic clocks," Electron. Lett. **51**, 1767–1769 (2015).
[23]G. J. Dick, "Local oscillator induced instabilities in trapped ion frequency standards," in *Proceedings of 19th Precise Time and Time Interval Meeting*, Redondo Beach, CA (1987), pp. 133–147; G. Santarelli, C. Audoin, A. Makdissi, P. Laurent, G. J. Dick, and A. Clairon, "Frequency stability degradation of an oscillator slaved to a periodically interrogated atomic resonator," IEEE Trans. Ultrason. Ferroelectr. Freq. Control **45**, 887–894 (1998).